Luminescent Star-Shaped Zinc(II) and Platinum(II) Complexes Based on Star-Shaped 2,2′-Dipyridylamino-Derived Ligands

Corey Seward,[a] Jun Pang,[a] and Suning Wang*[a]

Keywords: Starburst molecules / Zinc / Platinum / N ligands / Luminescence

New Zn^{II} and Pt^{II} complexes of the star-shaped ligands 2,4,6-tris(2,2′-dipyridylamino)-1,3,5-triazine (tdat), 1,3,5-tris(2,2′-dipyridylamino)benzene (tdab), 2,4,6-tris[*p*-(2,2′-dipyridylamino)phenyl]-1,3,5-triazine (tdapt) and 1,3,5-tris[*p*-(2,2′-dipyridylamino)phenyl]benzene (tdapb) have been synthesized and characterized. 1:1, 1:2 and 1:3 (ligand vs. the number of Zn atoms) Zn^{II} complexes of the tdat ligand have been identified. The 1:1 and 1:2 Zn^{II} complexes of tdat are dynamic in solution. For the tdab, tdapt and tdapb ligands, only 1:3 complexes of Pt^{II} and Zn^{II} have been isolated. Single-crystal X-ray diffraction analyses have been carried out for some of these new complexes, which revealed that there is a distinct difference in the arrangement of star-shaped ligands in the complexes of Zn^{II} and those of Pt^{II}. The Pt^{II} complexes of tdat and tdab adopt an unusual "bowl" shape and stack in a "head-to-tail" fashion in the crystal lattice. In contrast, the corresponding Zn^{II} complexes do not have a "bowl" shape. The difference between the Zn^{II} complexes and the Pt^{II} complexes can be attributed to the different coordination geometry preferred by the two metal ions. The Zn^{II} complex of tdapb displays several crystal motifs, two of which contain benzene molecules in the crystal lattices. All complexes are luminescent in the blue region, attributable to ligand-based $\pi \rightarrow \pi^*$ transitions.

Introduction

Luminescent metal complexes are a fascinating class of molecules that have found applications in many areas of chemistry and materials science. For example, it has been demonstrated recently that luminescent metal compounds can function as emitters in light emitting devices (LEDs).[1] Luminescent compounds have been used widely as sensors and probes for a variety of chemical and biological substances.[2] Luminescent transition metal compounds have also been demonstrated as models/centers for photochemical devices/reactions.[3] There is an increasing demand for new luminescent metal compounds that can perform one or two desired functions, such as emitting light in organic LEDs or detecting certain molecules of environmental concern. Toward that goal, recently we developed a class of blue luminescent star-shaped organic molecules of 2,2′-dipyridylamino derivatives based on 2,4,6-trisubstituted triazine and 1,3,5-trisubstituted benzene (Scheme 1) that have been found to be promising blue emitters in organic LEDs.[4] Star-shaped luminescent organic molecules have been explored extensively as either emitters or host materials in organic LEDs due to their good film-forming properties.[5] The corresponding luminescent star-shaped metal complexes may offer new properties that are not present in the organic molecules. For example, in a recent preliminary communication we reported that the star-shaped ligand tdapb {tdapb = 1,3,5-tris[*p*-(2,2′-dipyridylamino)phenyl]-benzene} forms a 1:3 complex with $ZnCl_2$ that is blue luminescent and has a highly selective fluorescent response toward benzene.[6] The highly selective fluorescent response of the zinc star-shaped complex was attributed to the extended molecular architecture in the crystal lattice. We have now extended our investigation to metal complexes of other members of our star-shaped ligands and Pt^{II} complexes. Unlike the Zn^{II} ion, which prefers a tetrahedral geometry, the Pt^{II} ion adopts a square-planar geometry. Consequently, it is anticipated that the molecular shape of Pt^{II} complexes will be quite different from those of the corresponding Zn^{II} complexes. Furthermore, Pt^{II} centers tend to enhance phosphorescence but quench fluorescence from the ligand, due to their d^8 electronic configuration. The replacement of Zn^{II} ions by Pt^{II} ions in the complex could therefore lead to a significant change of luminescent properties. Some interesting molecular and extended structural variations and dynamic behaviors in solution have been observed in the new complexes. In the present paper, we give a full account on the results of our comparative study on syntheses, structures and luminescent properties of Zn^{II} and Pt^{II} complexes with the four star-shaped ligands listed in Scheme 1.

[a] Department of Chemistry, Queen's University, Kingston, Ontario, K7L 3N6, Canada
wangs@chem.queensu.ca

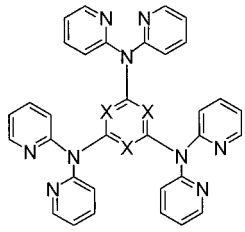

X = CH, tdab; X = N, tdat

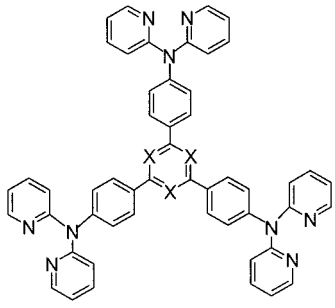

X = CH, tdapb; X = N, tdapt

Scheme 1

Results and Discussion

Syntheses and Structures

Zn^{II} Complexes of 2,4,6-Tris(2,2′-dipyridylamino)-1,3,5-triazine (tdat) and 1,3,5-Tris(2,2′-dipyridylamino)benzene (tdab)

The Zn^{II} complexes of tdat and tdab were obtained from the reactions of $ZnCl_2$ with the corresponding ligand in either CH_2Cl_2/THF solution or CH_2Cl_2/methanol solution. For the tdat ligand, by controlling the stoichiometry of the reaction, three Zn^{II} complexes, $(ZnCl_2)$(tdat) (**1a**), $(ZnCl_2)_2$(tdat) (**1b**), and $(ZnCl_2)_3$(tdat) (**1c**) with a tdat ligand/Zn^{II} ratio of 1:1, 1:2 and 1:3, respectively, were obtained and characterized. However, for the tdab ligand, only the 1:3 complex $(ZnCl_2)$(tdab) (**2**) was isolated, regardless of the ratio of the tdab ligand to $ZnCl_2$ employed in the reaction. The tdat and tdab Zn^{II} complexes are all stable under air in solution and in the solid state. Except for **1a**, these complexes are scarcely soluble in common organic solvents. Compounds **1a**−**1c** and **2** were characterized by ^{1}H NMR spectroscopy and elemental analyses. Single crystals of **1b** and **2**, suitable for X-ray diffraction analyses were obtained and their structures were determined by X-ray diffraction experiments. The crystal structures of **1b** and **2** are shown in Figures 1 and 2, respectively. Selected bond lengths and angles are given in Table 1.

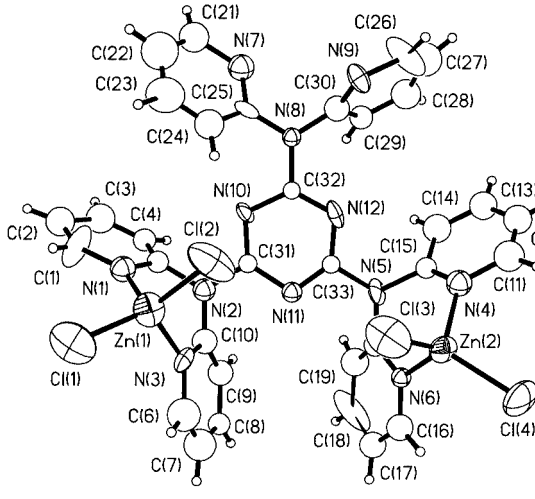

Figure 1. Molecular structure of **1b** with 50% thermal ellipsoids and labeling schemes

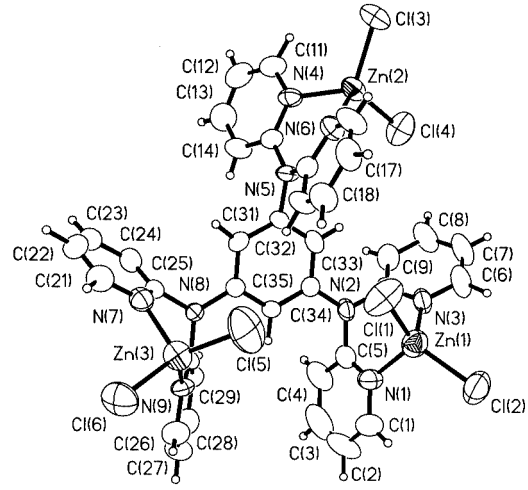

Figure 2. Molecular structure of **2** with 50% thermal ellipsoids and labeling schemes

As shown by Figure 1, the two $ZnCl_2$ units are chelated by two of the dipyridylamino groups in the tdat ligand in **1b** with a typical tetrahedral geometry and normal bond lengths.[7] The third dipyridylamino group does not coordinate. The two $ZnCl_2$ units are on the same side with respect to the triazine ring. The Zn(1)−Zn(2) distance is 7.302(2) Å. Based on the structure of **1b**, we can assume that in the 1:1 complex **1a** the $ZnCl_2$ unit is chelated by the dipyridylamino group in the same manner as observed in **1b**. Because of the existence of both coordinated and noncoordinated dipyridylamino groups in **1b**, one would expect that three sets of chemical shifts for the pyridyl groups (the two pyridyl groups bound to the Zn^{II} ion are not equivalent) should be observed in the ^{1}H NMR spectrum of **1b**. Similarly, three sets of chemical shifts for the pyridyl groups a, b and c (see Scheme 2) are expected for compound **1a**. However, at ambient temperature only one set of pyridyl chemical shifts was observed for both compounds **1a** and **1b**, which leads us to believe that there is a dynamic exchange for compounds **1a** and **1b** in solution. Compound **1b** does not have appreciable solubility in common organic solvents such as CH_2Cl_2, $CHCl_3$ or THF, precluding any low-temperature

Table 1. Range of selected bond lengths [Å] and angles [°] for **1b**, **2**−**4**, **6a** and **6b**

	M−Cl range	M−N range	C−N range	C−C range
1b	2.190(6)−2.221(5)	1.977(14)−2.067(13)	1.274(16)−1.447(19)	1.27(2)−1.46(2)
2	2.2820(17)−2.2209(16)	2.017(4)−2.075(4)	1.331(5)−1.438(5)	1.344(8)−1.411(9)
3	2.273(8)−2.331(8)	2.041(19)−2.07(2)	1.22(2)−1.48(3)	1.24(4)−1.55(4)
4	2.284(3)−2.286(3)	2.018(8)−2.025(8)	1.325(12)−1.464(17)	1.302(17)−1.393(12)
6a	2.190(3)−2.198(3)	2.017(8)−2.051(8)	1.315(11)−1.467(10)	1.321(16)−1.512(11)
6b	2.148(4)−2.212(3)	1.9696(11)−2.052(9)	1.326(12)−1.473(11)	1.336(15)−1.526(12)
	Cl−M−Cl range	Cl−M−N range	N−M−N range	
1b	120.0(2)−121.5(2)	105.2(5)−114.2(4)	88.4(6)−91.4(5)	
2	117.97(7)−123.05(7)	102.51(13)−118.16(13)	87.95(16)−89.00(17)	
3	89.3(3)−91.3(4)	89.6(6)−179.4(7)	89.0(8)−90.6(10)	
4	90.0(3)−91.29(12)	89.9(2)−178.4(2)	87.4(5)−87.8(3)	
6a	116.85(16)−117.24(14)	108.0(2)−116.4(2)	90.4(3)−90.6(3)	
6b	119.58(15)−122.80(14)	105.2(3)−116.0(3)	88.8(5)−90.1(4)	
	C−N−C range	C−C−N range	C−C−C range	
1b	111.7(15)−121.9(16)	116(2)−127.7(18)	111(2)−125(2)	
2	115.8(4)−126.5(4)	117.7(5)−124.6(6)	115.4(5)−121.5(5)	
3	112(3)−128(2)	116(3)−125(3)	115(3)−127(3)	
4	114.7(11)−122.8(7)	118.4(6)−123.5(8)	118.4(9)−123.2(12)	
6a	116.0(7)−127.8(7)	117.3(8)−125.6(10)	116.1(11)−124.3(11)	
6b	113.9(9)−129.5(9)	116.0(11)−128.2(12)	114.7(15)−123.6(12)	

NMR experiments. Compound **1a** has a sufficient solubility in CH_2Cl_2 and allows us to carry out variable-temperature ^{1}H NMR experiments. The ^{1}H NMR spectra of **1a** over the temperature range of 180−298 K recorded in CD_2Cl_2 are shown in Figure 3, which confirms the existence of dynamic exchange of **1a** in solution. If compound **1a** retains its structure as shown in Scheme 2, twelve chemical shifts corresponding to three sets of pyridyl groups should be observed in the ^{1}H NMR spectrum of **1a**. The 180 K spectrum of **1a** displays eleven reasonably resolved peaks with some overlaps, indicating that **1a** indeed retains the expected structure in solution at low temperature. However, at ambient temperature, it undergoes a rapid exchange process, which might be attributed to an intramolecular "merry-go-round" by the $ZnCl_2$ unit as shown by Scheme 2. Alternatively, an intermolecular process that involves the dissociation of $ZnCl_2$ from the ligand and the reattachment to the ligand is also possible. Given the fact that no intermolecular exchange was observed in our previously reported Zn^{II} complexes involving dipyridyl chelate ligands,[8] we believe that the intramolecular process is most likely responsible for the dynamic exchange of **1a**. A similar exchange process is also believed to be responsible for the observed dynamic behavior of **1b**.

As shown in Figure 2, the three $ZnCl_2$ units in compound **2** are all chelated by dipyridylamino groups in the same manner as observed for compound **1b**. Two of the $ZnCl_2$ units are on the same side with respect to the central phenyl ring. However, the third $ZnCl_2$ unit is nearly parallel to the central phenyl ring with the two attached pyridyl rings above and below, respectively. The Zn(1)−Zn(3) separation distance of 7.148(2) Å − the shortest Zn−Zn distance in **2** [Zn(1)−Zn(2) = 7.602(2) Å, Zn(2)−Zn(3) = 9.376(1) Å] − is considerably shorter than that of **1b**. The tdat 1:3 complex **1c** is believed to have a structure similar to **2**.

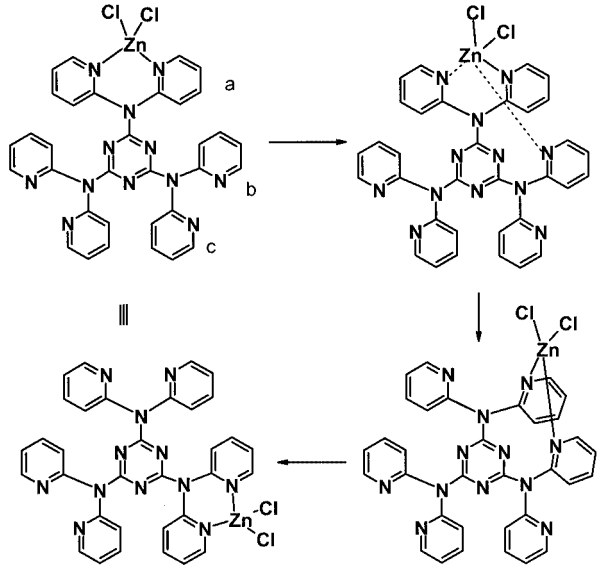

Scheme 2

Pt^{II} Complexes of tdat and tdab

The light yellow 1:3 Pt^{II} complexes of tdat and tdab, **3** and **4**, were obtained from the reactions of the corresponding ligands with K_2PtCl_4 in a 1:3 ratio by using a solvent-layering/slow diffusion method. This procedure is necessary to obtain sufficiently large single crystals of **3** and **4** for X-

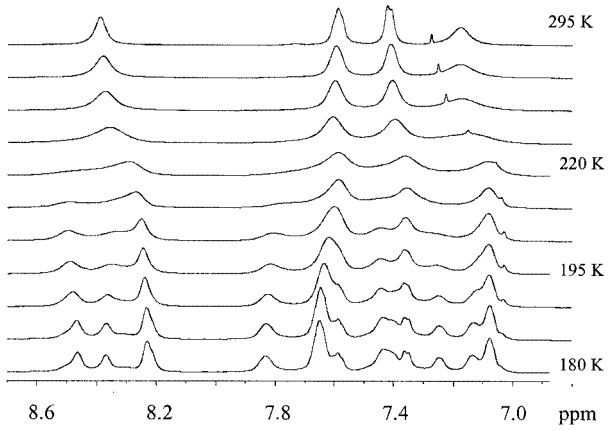

Figure 3. Variable-temperature ^{1}H NMR spectra of **1a** in CD_2Cl_2

ray diffraction analyses, due to the insolubility of the resulting complexes in organic solvents. Compounds **3** and **4** are stable in air. Because of the insolubility of **3** and **4** in organic solvents such as CH_2Cl_2 and DMSO, we were unable to obtain their ^{1}H NMR spectra. These two compounds were characterized by elemental analyses and single-crystal X-ray diffraction analyses. The structures of **3** and **4** are shown in Figures 4 and 6, respectively. Selected bond lengths and angles are listed in Table 1.

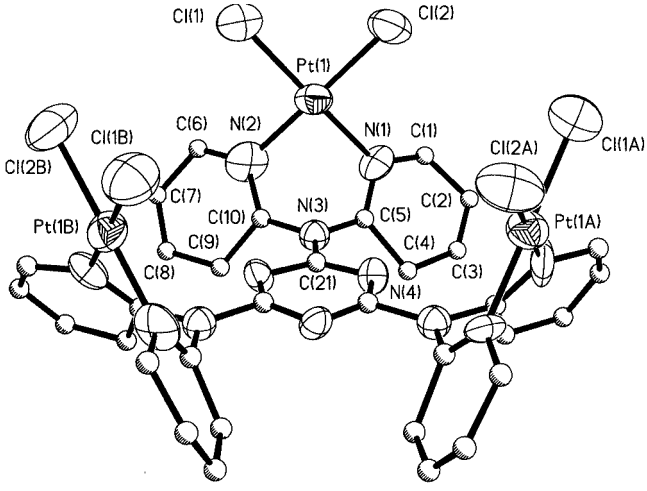

Figure 4. Molecular structure of one of the independent molecules of **3** with 50% thermal ellipsoids and labeling schemes; hydrogen atoms were omitted for clarity and carbon atoms are shown as ideal spheres

Compound **3** crystallizes in two different crystal lattices, hexagonal $R3c$ and monoclinic $P2_1/m$. The monoclinic form of **3** is isomorphous with that of **4**. Therefore, the discussion here focuses on the hexagonal form. There are two independent molecules of **3** in the asymmetric unit cells with similar structures. One of the independent molecules is shown in Figure 4. The three $PtCl_2$ groups in **3** are chelated by dipyridylamino units, resulting in a square-planar geometry for each of the Pt^{II} centers. The Pt−Cl and Pt−N bond lengths in **3** are normal.[3,9] Each molecule of **3** has a crystallographically imposed C_3 rotation symmetry. The intramolecular Pt−Pt separation distances of **3** are 7.710(2) Å and 7.570(2) Å, respectively, for the two independent molecules. The most remarkable feature of **3** is that all three $PtCl_2$ units are oriented on the same side of the triazine ring, thus forming a "bowl-shaped" structure. The absence of the "bowl" structure for compound **2** can be explained by the fact that this would bring the chloride ligands into close contact with each other because of the tetrahedral geometry of the Zn^{II} ion. The second remarkable feature of **3** is that the molecules of **3** stack in the crystal lattice along the C_3 axis, like a stack of bowls (Figure 5). The two neighboring molecules within the stack are rotated by about 40° with respect to each other, resulting in the formation of a polar column. Furthermore, these stacks of **3** are oriented to the same direction, thus resulting in the formation of the polar crystal lattice. The polar axial stacking of **3** could be attributed to intermolecular electrostatic interactions between the electronegative chloride ligands and the electropositive protons of the tdat ligand. The shortest intermolecular separation distance between the chlorine atom and the carbon atoms of the tdat ligand is 3.66 Å. The polar molecular stacking in the crystal lattice as displayed by compound **3** is quite uncommon and very interesting since it may lead to some unusual physical properties (i.e. nonlinear optical properties). We have not been able to

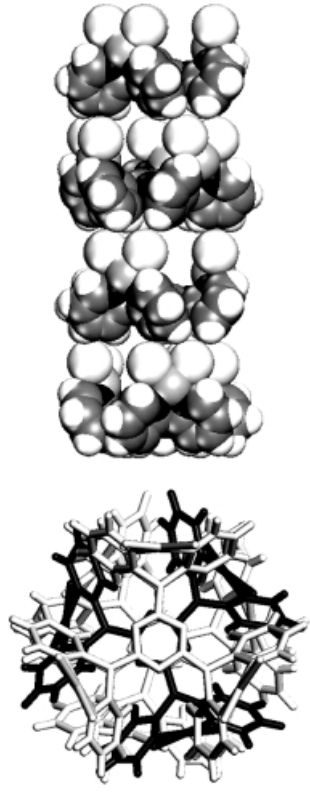

Figure 5. View of the stacking column of **3** projected along the C_3 axis (space-filling), and a view of the stacking column of **3** projected down the C_3 axis (stick)

study the optical/physical properties of the needle-like single-crystals of **3** because of their small sizes (< 0.1 mm in diameter).

The monoclinic form of compound **4** was identified and belongs to the centric monoclinic space group $P2_1/m$ with a crystallographically imposed mirror plane, upon which Pt(1), N(2), C(16) and C(19) lie. The structure of **4** is similar to that of **3**, except that the intramolecular Pt−Pt separation distances [8.271(2) Å, 8.279(2) Å] are much longer than those of **3** [the Pt−Pt separation distances of **3** in the $P2_1/m$ lattice are 7.829(2) Å and 8.069(2) Å], which could be attributed to the protons on the central phenyl ring in **4** that cause greater nonbonding interactions between the central phenyl ring and the pyridyl groups, compared to **3**. The major difference between the hexagonal form of **3** and the monoclinic form of **3** or **4** is the crystal lattice packing. In the crystal lattice of **4**, instead of stacking directly upon each other, the molecules are stacked in a "stair" fashion with a head-to-tail arrangement. In addition, the stacks of the molecules of **4** are oriented in two opposite directions as shown in Figure 6, thus resulting in a nonpolar crystal lattice. In the crystal lattices of **3** and **4** solvent molecules such as CH_2Cl_2 and H_2O were found, some of which were found to be trapped within the stacked column or inside the "bowl" of the Pt^{II} complex.

Zn^{II} Complexes of 2,4,6-Tris[p-(2,2′-dipyridylamino)-phenyl]-1,3,5-triazine (tdapt) and 1,3,5-Tris[p-(2,2′-dipyridylamino)phenyl]benzene (tdapb)

The colorless 1:3 zinc(II) complexes of tdapt and tdapb, namely $(ZnCl_2)_3$(tdapt) (**5**) and $(ZnCl_2)_3$(tdapb) (**6**) were obtained from the reactions of $ZnCl_2$ with the corresponding ligands in a 3:1 ratio in CH_2Cl_2/methanol solution. Both compounds are air-stable and have moderate solubility in organic solvents and have been characterized by elemental analyses and ^1H NMR spectroscopy. Attempts to obtain single crystals of **5** for X-ray diffraction analysis were unsuccessful. Compound **6** displays three different crystal motifs, depending on the solvent and the amount of each solvent used during crystallization. The first motif belongs to hexagonal space group $R\bar{3}$ with the formula $(ZnCl_2)_3$(tdapb)·$0.25C_6H_6$·$3CH_2Cl_2$ (**6a**), obtained from the solution of CH_2Cl_2 with a small amount of benzene. The second and third motifs belong to the triclinic space group $P\bar{1}$ with the formula $(ZnCl_2)_3$(tdapb)·$3C_6H_6$ (**6b**) and $(ZnCl_2)_3$(tdapb)·H_2O (**6c**), obtained from a solution of 1:1 CH_2Cl_2/benzene, and a methanol solution, respectively. Each of the crystal motifs was investigated by X-ray diffraction. The details of crystal structures of **6a** and **6b** are presented here. The molecular structure of the $(ZnCl_2)_3$(tdapb) molecule in all three motifs is similar, with an approximate C_3 symmetry. The C_3 symmetry for **6a** as shown in Figure 7 is rigorously imposed by the crystal symmetry. The molecular structure of compound **5** is believed to be similar to that of **6**. In the same manner as observed for compounds **1b** and **2**, the three $ZnCl_2$ units in compound **6** are chelated by the dipyridylamino groups with a typical tetrahedral geometry. The three $ZnCl_2$ units in **6a** are all on the same side with respect to the central phenyl ring. In the crystal lattice of **6a**, the two nearest molecules of **6** are paired and staggered in a *face-to-face* fashion with an intermolecular separation between the central phenyl rings of 3.85(1) Å. These pairs stack along the *c* axis to form a hexagonal column. As shown in Figure 8, a benzene molecule is situated directly above the central phenyl ring and sandwiched by two pairs of the Zn^{II} complex. The separation distance between the benzene molecule and the two central phenyl rings of **6** is 3.60(1) Å, indicative of the presence of π−π stacking interactions.

Figure 6. Stick diagram showing the stacking of **4** in the crystal lattice

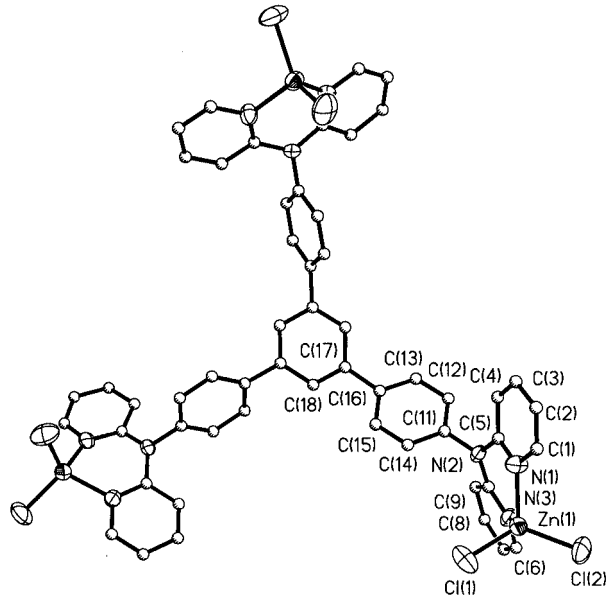

Figure 7. Molecular structure of one of the independent molecules of **6a** with 50% thermal ellipsoids and labeling schemes; hydrogen atoms are omitted for clarity; carbon atoms are shown as ideal spheres

There are three benzene solvent molecules per molecule of **6** in the crystal lattice of **6b**, which do not stack with the Zn^{II} complex in the *face-to-face* manner as observed in **6a**. Two of the benzene molecules are nearly perpendicular to the tdapb ligand while the remaining one is somewhat parallel to the tdapb ligand, but is perpendicular to a neighbor-

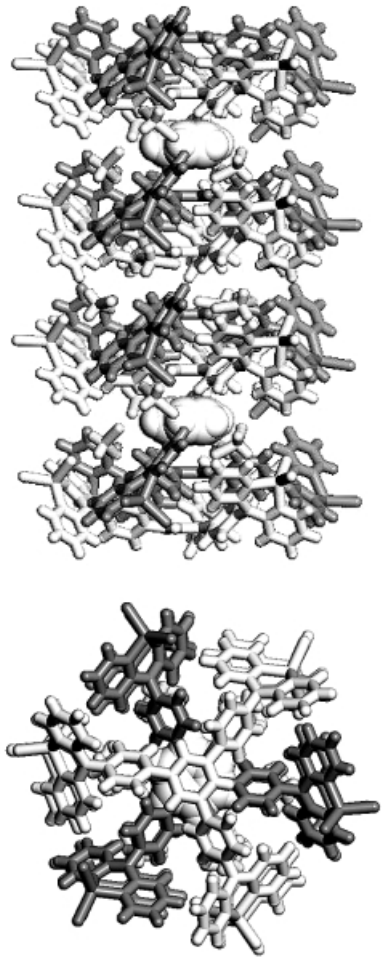

Figure 8. Diagram showing the pairing of **6a** (light gray and dark gray) and its stacking with benzene (space-filling) projected along the C_3 axis (left) and down the C_3 axis (right)

ing tdapb ligand of an adjacent molecule in the lattice. The π-π interactions in **6b** are therefore both *edge-to-face* and *face-to-face*.[10] The benzene solvent molecules are all located in the channels of the crystal lattice as shown by the unit cell packing diagram in Figure 9. The crystals of **6a** and **6b** indicate that compound **6** has a high affinity toward benzene in the solid state. In a recent report, we demonstrated that compound **6** is a highly selective fluorescent sensor for benzene vapor,[6] attributable to the high affinity of compound **6** in the solid state toward benzene. The free ligand tdapb is not effective as a fluorescent sensor for benzene, despite its bright blue luminescence. We believe that the coordination of the Zn^{II} ions to the tdapb ligand makes possible the formation of extended architectures in the solid state that attract benzene molecules and allow them to interact with the luminescent center effectively.

Pt^{II} Complexes of tdapt and tdapb

The 1:3 Pt^{II} complexes of tdapt and tdapb, namely $(PtCl_2)_3$(tdapt) (**7**) and $(PtCl_2)_3$(tdapb) (**8**) were obtained by using the same procedure as employed for **3** and **4**. Compounds **7** and **8** are insoluble in organic solvents, which precluded their study by solution NMR spectroscopy. Both

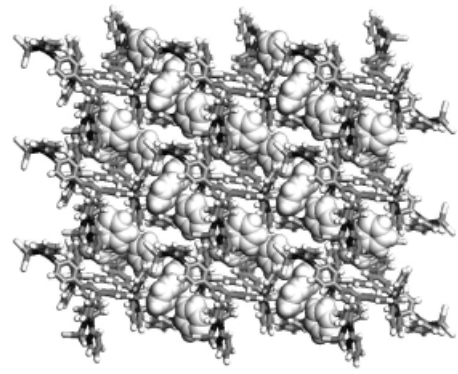

Figure 9. Unit cell packing diagram projected down the *b* axis; the benzene solvent molecules are highlighted as space-filling models

compounds form very thin, hair-like light yellow needles, too small for X-ray diffraction studies. Their compositions were confirmed by elemental analyses. We believe that the three $PtCl_2$ units in **7** and **8** are chelated by the dipyridylamino groups of the tdapt or tdapb ligand in the same manner as observed for compounds **3** and **4**.

Luminescent Properties

The free ligands tdat, tdab, tdapt and tdapb are blue-luminescent with a high quantum efficiency.[4] The nature of the emission of the free ligands is fluorescent, attributable to π→π* transitions. The Zn^{II} and Pt^{II} complexes of these ligands have also been found to be luminescent with broad emission bands that cover most of the blue region and resemble those of the free ligands. Therefore, we believe that the observed luminescence of the Zn^{II} and Pt^{II} complexes are ligand-based π→π* transitions localized mostly on the dipyridylamino chromophore. The luminescent intensity of the complexes is in general much weaker than that of the corresponding free ligand. For the Zn^{II} complexes, the decrease of luminescent intensity can be attributed to the chloride ligand, which is known to quench fluorescence through "heavy atom effects". The decrease of luminescent intensity of the Pt^{II} complexes can be attributed to the Pt^{II} center, which is an effective quencher of ligand fluorescence. No significant phosphorescence was observed for the Pt^{II} complexes. The luminescent data were obtained in solution and in the solid state for most of the Zn^{II} complexes. Because of their insolubility in organic solvents, only luminescent data in the solid state were obtained for the Pt^{II} complexes. For comparison purposes, the emission data of the free ligands (the details of luminescent data for the free ligands can be found in ref.[4]) are listed in Table 2, along with the luminescent data of the complexes. As a representative example, the emission spectra of tdapb and its Zn^{II} and Pt^{II} complexes **6** and **8** in the solid state are shown in Figure 10. The emission spectra of tdat and tdapt complexes are in general much broader than those of tdab and tdapb complexes. The contribution of the central triazine ring to the emission is likely to be responsible for the broad emission band. As shown in Table 2, the Zn^{II} complexes of tdab and tdapb show a significant red shift of

Table 2. Luminescence data

	Solution (CH_2Cl_2)			Solid	
	Excitation (λ_{max})	Emission (λ_{max})	Φ	Excitation (λ_{max})	Emission (λ_{max})
tdat	371	433	0.43	397	469
$(ZnCl_2)$(tdat) (**1a**)	295	418	0.011		
$(ZnCl_2)_2$(tdat) (**1b**)	292	399	0.08		
$(ZnCl_2)_3$(tdat) (**1c**)	292	318, 378	0.038	318	380
$(PtCl_2)_3$(tdat) (**3**)				346	414
tdab	385	412	0.53	387	412
$(ZnCl_2)_3$(tdab) (**2**)	316	426	0.097	385	447
$(PtCl_2)_3$(tdab) (**4**)				347	411
tdapt	420	440	0.78	423	461
$(ZnCl_2)_3$(tdapt) (**5**)	358	445	0.15	446	505
$(PtCl_2)_3$(tdapt) (**7**)				323	390
tdapb	367	384	0.16	380	409
$(ZnCl_2)_3$(tdapb) (**6**)	331	464	0.089	381	432
$(PtCl_2)_3$(tdapb) (**8**)				324	376

emission energy in solution, in comparison to the free ligands, which is consistent with our previously reported Zn^{II} complexes of tripyridylamines where two of the pyridyl groups are chelated to the Zn^{II} center and a similar red shift was observed.[7] The most dramatic red shift was displayed by the tdapt complex **5** which has an emission maximum at 505 nm in the solid state, even though it does not display a significant red shift in solution. This red shift is believed to be associated with intermolecular interactions of **5** in the solid state, but the details are not understood due to the lack of crystal data for **5**.

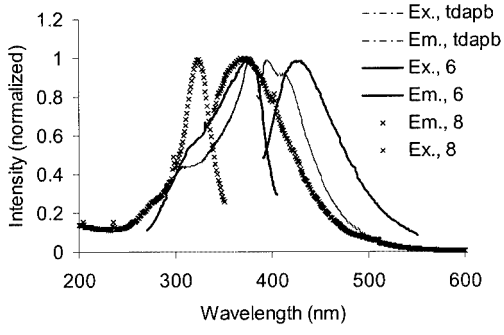

Figure 10. Excitation and emission spectra of tdapb, **6** and **8** in the solid state

For the Zn^{II} complex **6**, we examined the luminescent spectra of the three different crystal forms in the solid state, which revealed that there is no significant difference between their excitation or emission spectra. The exposure of complex **6** in the solid state or in a [poly(dimethylsiloxane)] (PDMS) matrix to a benzene vapor causes a decrease in emission intensity, attributable to fluorescent quenching via π−π interactions between benzene molecules and the complex (the details of the use of **6** as a fluorescent sensor for benzene can be found in ref.[4]). Blue-luminescent compounds are ideal for the detection of aromatic organic molecules because most aromatic organic molecules absorb strongly in the UV or near UV region. Therefore, in addition to the studies of **6**, systematic studies on the potential of the Zn^{II} complexes **1**, **2** and **5** as fluorescent sensors for aromatic organic solvent molecules are being carried out by our group and the results will be reported in due course.

The Pt^{II} complexes **3**, **4**, **7** and **8** have a broad emission band that is either similar to that of the free ligand or blue-shifted. The luminescent intensity of the Pt^{II} complexes in the solid state is clearly much weaker than those of the corresponding Zn^{II} compounds, attributable to fluorescent quenching by the Pt^{II} centers. Compounds **3** and **4** appear to have the tendency to attract small halogenated solvent molecules such as CH_2Cl_2 into their crystal lattices, as demonstrated by their crystal structural analyses. The effect of halogenated solvent molecules on the luminescence of compounds **3** and **4** in the solid state and the potential use of **3** and **4** as fluorescent sensors for halogenated molecules are being investigated.

In summary, we have demonstrated that the star-shaped ligands of tdat, tdab, tdapt and tdapb are capable of chelating to Zn^{II} and Pt^{II} centers to form a new class of luminescent star-shaped complexes. These complexes display interesting and unusual structural features and molecular arrangements in the solid state. Due to their low emission efficiency and poor volatility and solubility, these complexes are not suitable for electroluminescent applications. However, some of these complexes appear to have a high affinity toward certain organic solvent molecules and may find use as fluorescent sensors for these molecules.

Experimental Section

General: $ZnCl_2$ and K_2PtCl_4 were purchased from Strem Chemicals Co. Solvents were freshly distilled from appropriate drying reagents prior to use. ^1H NMR spectra were recorded by using Bruker Avance 300 MHz spectrometers. Elemental analyses were performed by Canadian Microanalytical Service, Ltd., Delta, British Columbia. Excitation and emission spectra were recorded with a Photon Technologies International QuantaMaster Model C-60 spectrometer. Melting points were determined with a Fisher−Johns melting point apparatus. The tdat, tdab, tdapt and tdapb ligands were synthesized based on the procedure reported recently.[4] All Pt^{II}

complexes reported herein are insoluble in common organic solvents. ^{1}H NMR spectra for these compounds are therefore not provided.

Synthesis of $(ZnCl_2)$(tdat) (1a): Zinc chloride (12 mg, 0.085 mmol) was dissolved in THF (10 mL); tdat (50 mg, 0.085 mmol) in 10 mL of CH_2Cl_2 was added to the zinc chloride solution at ambient temperature. The solution was stirred for 0.5 h. After the solution was allowed to stand for a few days, a colorless crystalline solid of $(ZnCl_2)$(tdat) was obtained (45 mg, yield 73%). ^{1}H NMR (CD_3OD, 298 K): δ = 8.28 (d, ^3J = 3.9 Hz, 6 H, py), 7.75 (dd, $^3J_1$ = 8.1, $^3J_2$ = 6.6 Hz, 6 H, py), 7.51 (d, ^3J = 8.4 Hz, 6 H, py), 7.21 (dd, $^3J_1$ = 7.2, $^3J_2$ = 4.8 Hz, 6 H, py). $C_{33}H_{24}Cl_2N_{12}Zn$ (724.29): calcd. C 54.67, H 3.34, N 23.19; found C 54.18, H 3.46, N 22.71.

Synthesis of $(ZnCl_2)_2$(tdat) (1b): Zinc chloride (23 mg, 0.17 mmol) was dissolved in THF (10 mL); tdat (50.0 mg, 0.085 mmol) in 10 mL of CH_2Cl_2 was added to the zinc chloride solution at ambient temperature. The solution was stirred for 0.5 h. After the solution was allowed to stand for a few days, a colorless crystalline solid of $(ZnCl_2)_2$(tdat) was obtained (37 mg, yield 50%). ^{1}H NMR ([D$_6$]DMSO, 298 K): δ = 8.24 (d, ^3J = 4.8 Hz, 6 H, py), 7.68 (dd, $^3J_1$ = 8.1, $^3J_2$ = 5.7 Hz, 6 H, py), 7.46 (d, ^3J = 8.1 Hz, 6 H, py), 7.12 (dd, $^3J_1$ = 5.7, $^3J_2$ = 4.8 Hz, 6 H, py). $C_{33}H_{24}Cl_4N_{12}Zn_2$ (860.58): calcd. C 46.02, H 2.81, N 19.52; found C 45.38, H 2.98, N 19.21.

Synthesis of $(ZnCl_2)_3$(tdat) (1c): Zinc chloride (35 mg, 0.255 mmol) was dissolved in THF (10 mL); tdat (50 mg, 0.085 mmol) in 10 mL of CH_2Cl_2 was added to the zinc chloride solution at ambient temperature. The solution was stirred for 0.5 h. After the solution was allowed to stand for a few days, a colorless crystalline solid of $(ZnCl_2)_3$(tdat) was obtained (62 mg, yield 74%). ^{1}H NMR ([D$_6$]DMSO, 298 K): δ = 8.24 (d, ^3J = 4.8 Hz, 6 H, py), 7.68 (dd, $^3J_1$ = 7.8, $^3J_2$ = 5.7 Hz, 6 H, py), 7.46 (d, ^3J = 8.1 Hz, 6 H, py), 7.12 (dd, $^3J_1$ = 5.7, $^3J_2$ = 4.8 Hz, 6 H, py). $C_{33}H_{24}Cl_6N_{12}Zn_3\cdot 1CH_2Cl_2\cdot 0.5THF$ (1117.77): calcd. C 38.64, H 2.68, N 15.02; found C 39.24, H 2.94, N 14.64.

Synthesis of $(ZnCl_2)_3$(tdab) (2): Zinc chloride (38 mg, 0.28 mmol) was dissolved in CH_3OH (10 mL); tdab (50 mg, 0.085 mmol) in 5 mL of CH_2Cl_2 was added to the zinc chloride solution at ambient temperature. The solution was stirred for 2 h. After the solution was allowed to stand for a few days at ambient temperature, a colorless crystalline solid of $(ZnCl_2)_3$(tdab) was obtained (64 mg, yield 75%). ^{1}H NMR ([D$_6$]acetone, 298 K): δ = 8.51 (d, ^3J = 5.4 Hz, 6 H, py), 8.08 (dd, $^3J_1$ = 9.0, $^3J_2$ = 6.9 Hz, 3 H, py), 7.63 (d, ^3J = 8.4 Hz, 6 H, py), 7.51 (dd, $^3J_1$ = 6.9, $^3J_2$ = 5.7 Hz, 6 H, py). 7.45 (s, 6 H, ph). $C_{36}H_{27}Cl_6N_9Zn_3\cdot 2CH_2Cl_2\cdot 3H_2O$ (1217.67): calcd. C 37.44, H 3.03, N 10.34; found C 37.20, H 2.46, N 10.66.

Synthesis of $[(PtCl_2)_3$(tdat)] (3): Benzene (4 mL) and a solution of K_2PtCl_4 (106 mg, 0.255 mmol) in a mixture of 3 mL of H_2O and 5 mL of DMSO were successively layered upon a solution of tdat (50 mg, 0.085 mmol) in 6 mL of CH_2Cl_2. The yellow K_2PtCl_4/H_2O/DMSO solution sank through the layer of benzene and settled upon the tdat/CH_2Cl_2 layer. The solvents were allowed to diffuse over several days at ambient temperature, yielding a yellow crystalline solid of $[(PtCl_2)_3$(tdat)] (52% yield). $C_{33}H_{24}Cl_6N_{12}Pt_3\cdot 1$DMSO (1466.68): calcd. C 28.65, H 2.04, N 11.46; found C 28.87, H 2.09, N 10.87.

Synthesis of $[(PtCl_2)_3$(tdab)] (4): Compound **4** was obtained in 38% yield by using the same procedure as for **3**. $C_{36}H_{27}Cl_6N_9Pt_3$ (1382.94): calcd. C 31.25, H 1.97, N 9.11; found C 31.25, H 2.25, N 8.95.

Synthesis of $(ZnCl_2)_3$(tdapt) (5): Zinc chloride (28 mg, 0.20 mmol) was dissolved in CH_3OH (10 mL); tdapt (50 mg, 0.061 mmol) in 5 mL of CH_2Cl_2 was added to the zinc chloride solution at ambient temperature. The solution was stirred for 2 h. After the solution was allowed to stand for a few days at ambient temperature, a colorless crystalline solid of $(ZnCl_2)_3$(tdapt) was obtained (39 mg, yield 42%). ^{1}H NMR ([D$_6$]DMSO, 298 k): δ = 8.67 (d, ^3J = 8.7 Hz, 6 H, py), 8.32 (d, ^3J = 8.7 Hz, 6 H, ph), 7.77 (dd, $^3J_1$ = 8.1, $^3J_2$ = 7.2 Hz, 6 H, py), 7.28 (d, ^3J = 8.7 Hz, 6 H, ph), 7.15 (dd, $^3J_1$ = 7.2, $^3J_2$ = 6.9 Hz, 6 H, py). 7.10 (d, ^3J = 8.1 Hz, 6 H, py). $C_{51}H_{36}Cl_6N_{12}Zn_3\cdot 0.5CH_2Cl_2$ (1267.32): calcd. C 48.76, H 2.91, N 13.25; found C 48.42, H 3.09, N 13.05.

Synthesis of $(ZnCl_2)_3$(tdapb) (6): A CH_2Cl_2 (5 mL) solution containing tdapb (50 mg, 0.061 mmol) was added to 10 mL of a CH_3OH solution containing $ZnCl_2$ (28 mg, 0.20 mmol) at ambient temperature; 10 mL of benzene was added to this solution. After stirring for 2 h, the mixture was allowed to stand for several days at ambient temperature. A colorless crystalline solid of $(ZnCl_2)_3$(tdapb) was obtained (58 mg, yield 76%). ^{1}H NMR ([D$_4$]methanol, 298 K): δ = 8.27 (d, ^3J = 5.1, 6 H, py), 7.90 (s, 3 H, Ph1), 7.86 (d, ^3J = 8.4 Hz, 6 H, Ph2), 7.77 (dd, $^3J_1$ = 6.3, $^3J_2$ = 2.1 Hz, 6 H, py), 7.31 (d, ^3J = 8.4 Hz, 6 H, Ph2), 7.14 (dd, $^3J_1$ = 5.1, $^3J_2$ = 2.1 Hz, 6 H, py), 7.11 (d, ^3J = 5.4 Hz, 6 H, py). $C_{54}H_{39}Cl_6N_9Zn_3\cdot 1/3C_6H_6$ (1247.87): calcd. C 53.85, H 3.20, N 10.10; found C 54.20, H 3.03, N 10.20. If the reaction was carried out in the absence of benzene and a small amount of benzene was added during the crystallization of **6**, the second crystal motif, $(ZnCl_2)_3$(tdapb)$\cdot 0.25C_6H_6\cdot 3CH_2Cl_2$, was obtained. $C_{54}H_{39}Cl_6N_9Zn_3\cdot 0.25C_6H_6\cdot 3CH_2Cl_2$ (1496.07): calcd. C 46.93, H 3.13, N 8.42; found C 46.61, H 2.94, N 8.80.)

Synthesis of $[(PtCl_2)_3$(tdapt)] (7) and $[(PtCl_2)_3$(tdapb)] (8): DMSO (2 mL), benzene (4 mL), and a solution of K_2PtCl_4 (76 mg, 0.184 mmol) in a mixture of 3 mL of H_2O and 5 mL of DMSO were successfully layered upon a solution of tdapt (50 mg, 0.061 mmol) or tdapb (50 mg, 0.061 mmol), respectively, in 6 mL of CH_2Cl_2. The Pt-containing solution sank through the benzene layer and into the DMSO layer and settled upon the tdapb or tdapt ligand layer in CH_2Cl_2. Solvents were allowed to diffuse over several days at ambient temperature, producing a yellow microcrystalline solid of $[(PtCl_2)_3$(tdapt)] (60% yield) and $[(PtCl_2)_3$(tdapb)] (95% yield), respectively. **7:** $C_{51}H_{36}Cl_6N_{12}Pt_3\cdot 1H_2O$ (1631.94): calcd. C 37.50, H 2.32, N 10.29; found C 37.19, H 2.39, N 10.09. **8:** $C_{54}H_{39}Cl_6N_9Pt_3\cdot 1CH_2Cl_2$ (1695.84): calcd. C 38.92, H 2.42, N 7.42; found C 38.52, H 2.61, N 7.48.

X-ray Crystallographic Analyses: Single crystals of **1b**, **2**−**4**, and **6** suitable for X-ray diffraction analyses were obtained. Attempts to obtain single crystals of the remaining compounds were unsuccessful. All crystals were mounted on glass fibers. Data were collected with a Bruker Smart CCD 1000 diffractometer with graphite-monochromated Mo-K_α radiation, operating at 50 kV and 35 mA at 23 °C, over a 2θ range of 3−57°. No significant decay was observed for any samples during the data collection. Data were processed with a Pentium III PC using the Bruker AXS SHELXTL NT software package. Neutral atomic scattering factors were taken from Cromer and Waber.[11] The crystals of **1b** were partially twinned and diffracted weakly. For compound **3**, two crystal motifs were observed, a hexagonal lattice and a monoclinic lattice. The monoclinic lattice of **3** is isostructural to that of **4** with unit cell dimensions of a = 9.9675(16), b = 21.356(4), c = 12.0891(19) Å, β = 98.532(4)°, V = 2544.9(7) Å^3. For compound **6**, three crystal motifs were observed, depending on the solvent used during crystallization. The unit cell parameters for two of the motifs **6a** and **6b** ob-

Table 3. Crystallographic data

	1b	**2**	**3**	**4**	**6a**	**6b**
	$(ZnCl_2)_2(tdat)\cdot H_2O$	$(ZnCl_2)_3(tdab)\cdot CH_3OH$	$(PtCl_2)_3(tdat)\cdot 1.5CH_2Cl_2\cdot H_2O$	$(PtCl_2)_3(tdab)\cdot 3CH_2Cl_2$	$(ZnCl_2)_3(tdapb)\cdot 0.25C_6H_6\cdot 3CH_2Cl_2$	$(ZnCl_2)_3(tdapb)\cdot 3C_6H_6$
Empirical formula	$C_{33}H_{24}Cl_4N_{12}Zn_2\cdot H_2O$	$C_{36}H_{27}Cl_6N_9Zn_3\cdot CH_3OH$	$C_{33}H_{24}Cl_6N_{12}Pt_3\cdot 1.5CH_2Cl_2\cdot H_2O$	$C_{36}H_{27}Cl_6N_9Pt_3\cdot 3CH_2Cl_2$	$C_{54}H_{39}Cl_6N_9Zn_3\cdot 0.25C_6H_6\cdot 3CH_2Cl_2$	$C_{54}H_{39}Cl_6N_9Zn_3\cdot 3C_6H_6$
Formula mass	879.20	1026.52	1532.01	1638.42	1497.06	1457.07
Space group	*Ia*	$P2_1/c$	*R*3*c*	$P2_1/m$	$R\bar{3}$	$P\bar{1}$
a [Å]	16.596(3)	8.2983(12)	22.471(4)	9.943(4)	33.517(4)	13.805(4)
b [Å]	14.208(3)	22.911(4)	22.471(4)	21.846(9)	$R\bar{3}$	14.848(5)
c [Å]	16.942(4)	21.869(3)	33.852(7)	12.163(5)	19.167(4)	17.384(5)
α [°]	90	90	90	90	90	87.208(6)
β [°]	107.473(4)	93.307(3)	90	97.575(8)	90	88.569(6)
γ [°]	90	90	120	90	120	77.828(8)
V [Å^3]	3810.5(14)	4150.9(11)	14803(5)	2618.8(19)	18647(4)	3478.7(18)
Z	4	4	12	2	12	2
μ [cm^{-1}]	15.85	21.49	90.13	86.44	8.8	13.04
$2\theta_{max.}$ [°]	56.7	56.6	56.6	56.7	56.6	57
Reflns. measured	13589	30012	33932	18966	46115	25315
Independent reflns.	7144 (R_{int} = 0.17)	9930(R_{int} = 0.086)	5717 (R_{int} = 0.132)	6391(R_{int} = 0.059)	10089 (R_{int} = 0.083)	16047 (R_{int} = 0.146)
Parameters	290	587	308	291	495	791
Final *R* [$I > 2\sigma(I)$]	R_1 = 0.1256[a], wR_2 = 0.1498[b]	R_1 = 0.0460[a], wR_2 = 0.0687[b]	R_1 = 0.0548[a], wR_2 = 0.1167[b]	R_1 = 0.0629[a], wR_2 = 0.1678[b]	R_1 = 0.1283[a], wR_2 = 0.3320[b]	R_1 = 0.0991[a], wR_2 = 0.1079[b]
Goodness of fit on F^2	0.772	0.740	0.922	1.065	1.136	1.136

[a] $R_1 = \Sigma\,||F_o|^2 - |F_c|^2|/\Sigma|F_o|^2$. [b] $wR_2 = \{\Sigma w[(F_o^2 - F_c^2)^2]/\Sigma[\,w(F_o^2)^2]\}^{1/2}$. $w = 1/[\sigma^2(F_o^2) + (0.075P)^2]$, where $P = [\max.(F_o^2,0) + 2F_c^2]/3$.

tained from benzene and CH_2Cl_2 solution are given in Table 3. The third motif **6c**, obtained from methanol solution, has the following unit cell parameters: triclinic, $P\bar{1}$, a = 13.134(9), b = 14.04(1), c = 16.67(1) Å, α = 73.01(1), β = 68.88(1), γ = 84.43(1)°, V = 2741(5) Å^3, Z = 2. The structure of **6c** is similar to that of **6b**, except that no benzene solvent molecules are present in the lattice. All structures were solved by direct methods. Almost all non-hydrogen atoms (except disordered solvent molecules) were refined anisotropically for all structures except compound **1b**. Due to the poor data quality of **1b**, only metal, chlorine and some nitrogen and carbon atoms could be refined anisotropically. Solvent molecules or H_2O were found in all crystals. Some of the solvent molecules are disordered. We invested considerable effort to model and refine the disordered solvent molecules. The positions for all hydrogen atoms except those of disordered solvent molecules or water molecules were either calculated or located directly from difference Fourier maps and their contributions to the structural factor calculation were included. The crystallographic data are given in Table 3. The ranges of selected bond lengths and angles are given in Table 1. CCDC-176676 (**1b**), -176678 (**2**), -176677 (**3**), -176675 (**4**), -163379 (**6a**), and -163380 (**6b**) contain the supplementary crystallographic data for this paper. These data can be obtained free of charge at www.ccdc.cam.ac.uk/conts/retrieving.html or from the Cambridge Crystallographic Data Centre, 12, Union Road, Cambridge CB2 1EZ, UK [Fax: (internat.) + 44-1223/336-033; E-mail: deposit@ccdc.cam.ac.uk].

Acknowledgments

We thank the Natural Sciences and Engineering Research Council of Canada and the Xerox Research Foundation for financial support.

[1] [1a] M. A Baldo, D. F. O'Brien, Y. You, A. Shoustikov, S. Sibley, M. E. Thompson, S. R. Forrest, *Nature* **1998**, *395*, 151. [1b] D. F. O'Brien, M. A. Baldo, M. E. Thompson, S. R. Forrest, *Appl. Phys. Lett.* **1999**, *74*, 442. [1c] R. C. Kwong, S. Sibley, T. Dubovoy, M. A. Baldo, S. R. Forrest, M. E. Thompson, *Chem. Mater.* **1999**, *11*, 3709. [1d] R. C. Kwong, S. Laman, M. E. Thompson, *Adv. Mater.* **2000**, *12*, 1134. [1e] C. J. Chen, J. Shi, *Coord. Chem. Rev.* **1998**, *171*, 161. [1f] N. X. Hu, M. Esteghamatian, S. Xie, Z. Popovic, A. M. Hor, B. Ong, S. Wang, *Adv. Mater.* **1999**, *11*, 17.

[2] [2a] M. A. Mansour, W. B. Connick, R. J. Lachicotte, H. J. Gysling, R. Eisenberg, *J. Am. Chem. Soc.* **1998**, *120*, 1329. [2b] Y. Kunugi, K. R. Mann, L. L. Miller, C. L. Exstrom, *J. Am. Chem. Soc.* **1998**, *120*, 589. [2c] E. Y. Fung, M. M. Olmstead, J. C. Vickery, A. L. Balch, *Coord. Chem. Rev.* **1998**, *171*, 151. [2d] J. C. Vickery, M. M. Olmstead, E. Y. Fung, A. L. Balch, *Angew. Chem. Int. Ed. Engl.* **1997**, *36*, 1179. [2e] G. De Santis, L. Fabbrizzi, M. Licchelli, A. Poggi, A. Taglietti, *Angew. Chem. Int. Ed. Engl.* **1996**, *35*, 202. [2f] A. P. de Silva, H. Q. N. Gunaratne, T. E. Rice, *Angew. Chem. Int. Ed. Engl.* **1996**, *35*, 2116. [2g] M. P. Houlne, T. S. Agent, G. F. Kiefer, K. McMillan, D. J. Bornhop, *Appl. Spectrosc.* **1996**, *10*, 225. [2h] K. H. Wong, M. C. W. Chan, C. M. Che, *Chem. Eur. J.* **1999**, *5*, 2845. [2i] W. Y. Wong, K. H. Choi, K. W. Cheah, *J. Chem. Soc., Dalton Trans.* **2000**, 113. [2j] H. Q. Liu, T. C. Cheung, C. M. Che, *Chem. Commun.* **1996**, 1039.

[3] [3a] W. Paw, S. D. Cummings, M. A. Mansour, W. B. Connick, D. K. Geiger, R. Eisenberg, *Coord. Chem. Rev.* **1998**, *171*, 125. [3b] S. D. Cummings, R. Eisenberg, *J. Am. Chem. Soc.* **1996**, *118*, 1949. [3c] S. Huertas, M. Hissler, J. E. McGarrah, R. J. Lachicotte, R. Eisenberg, *Inorg. Chem.* **2001**, *40*, 1183. [3d] M. Hissler, W. B. Connick, D. K. Geiger, J. E. McGarrah, D. Lipa, R. J. Lachicotte, R. Eisenberg, *Inorg. Chem.* **2000**, *39*, 447.

[4] J. Pang, Y. Tao, S. Freiberg, M. D'Iorio, S. Wang, *J. Mater. Chem.* **2002**, *12*, 206.

[5] [5a] N. Tamoto, C. Adachi, K. Nagai, *Chem. Mater.* **1997**, *9*, 1077. [5b] Z. Gao, C. S. Lee, L. Bello, S. T. Lee, R. M. Chen, T. Y. Luh, J. Shi, C. W. Tang, *Appl. Phys. Lett.* **1999**, *74*, 865. [5c] Y. Shirota, K. Okumoto, H. Inada, *Synth. Met.* **2000**, *111*, 387. [5d] S. Berleb, W. Brutting, M. Schwoerer, R. Wehrmann, A. Elschner, *J. Appl. Phys.* **1998**, *83*, 4403. [5e] K. Itano, T. Tsuzuki, H. Ogawa, S. Appleyard, M. R. Willis, Y. Shirota, *IEEE Trans. Electron. Devices* **1997**, *44*, 1218. [5f] Y. Kuwabara, H. Ogawa, H. Inada, N. Noma, Y. Shirota, *Adv. Mater.* **1994**, *6*, 677. [5g] I. Y. Wu, J. T. Lin, Y. T. Tao, E. Balasubramaniam, *Adv. Mater.* **2000**, *12*, 668.

[6] J. Pang, E. J. P. Marcotte, C. Seward, R. S. Brown, S. Wang, *Angew. Chem. Int. Ed.* **2001**, *40*, 4042.

[7] [7a] R. H. Prince, in *Comprehensive Coordination Chemistry* (Eds.: G. Wilkinson, R. D. Gillard, J. A. McCleverty), Pergamon Press, New York, **1987**, vol. 5, chapter 56.1. [7b] T. P. E. Auf der Heyde, *Acta Crystallogr., Sect. B* **1984**, *40*, 582. [7c] M. C. Kerr, H. S. Preston, H. L. Ammon, J. E. Huheey, J. M. Stewart, *J. Coord. Chem.* **1981**, *11*, 111. [7d] H. W. Smith, *Acta Crystallogr., Sect. B* **1975**, *31*, 2701. [7e] M. Mikami-Kido, Y. Saito, *Acta Crystallogr., Sect. B* **1982**, *38*, 452. [7f] Q. Wu, J. A. Lavigne, Y. Tao, M. D'Iorio, S. Wang, *Inorg. Chem.* **2000**, *39*, 5248;

[8] W. Yang, H. Schmider, Q. Wu, Y. Zhang, S. Wang, *Inorg. Chem.* **2000**, *39*, 2397.

[9] [9a] D. J. Cárdenas, A. M. Echavarren, *Organometallics* **1999**, *18*, 3337. [9b] G. W. V. Cave, N. W. Alcock, J. P. Rourke, *Organometallics* **1999**, *18*, 1801. [9c] M. J. Irwin, G. C. Jia, J. J. Vittal, R. J. Puddephatt, *Organometallics* **1996**, 5321.

[10] [10a] G. R. Desiraju, *Crystal Engineering: The Design of Organic Solids*, Elsevier, New York, **1989**. [10b] S. Tsuzuki, K. Honda, T. Uchimayu, M. Mikami, K. Tanabe, *J. Am. Chem. Soc.* **2002**, *124*, 104.

[11] D. T. Cromer, J. T. Waber, *International Tables for X-ray Crystallography*, Kynoch Press, Birmingham, AL, **1974**, vol. 4, Table 2.2A.

Received December 21, 2001
[I01528]